Characterization of an Alkaline Transition Intermediate Stabilized in the Phe82Trp Variant of Yeast *iso*-1-Cytochrome *c*[†]

Federico I. Rosell,[‡,§] Thomas R. Harris,[‡] Dean P. Hildebrand,[‡] Susanne Döpner,[‡,||] Peter Hildebrandt,[||] and A. Grant Mauk*[,‡]

Department of Biochemistry and Molecular Biology, University of British Columbia, Vancouver, British Columbia V6T 1Z3, Canada, and Max-Planck-Institute für Strahlenchemie, Stiftstrasse 34-36, D-45470 Mülheim an der Ruhr, Germany

Received May 12, 2000

ABSTRACT: In general, mutation of the phylogenetically conserved residue Phe82 in yeast *iso*-1-cytochrome *c* destabilizes the native conformation of the protein by facilitating the ligand exchange reactions that are associated with the alkaline conformational transitions of the ferricytochrome. Of the Phe82 variants surveyed thus far, Phe82Trp is unique in that it adopts a thermodynamically stable, high-spin conformation at mildly alkaline pH. This species exhibits spectroscopic features that can only be detected transiently in other ferricytochromes *c* within the first 100 ms immediately after a pH-jump from neutrality to pH >10. Spectroscopic characterization of this high-spin reaction intermediate suggests that in addition to an obligatory pentacoordinate heme iron, a group within the heme pocket coordinates the heme iron but is then replaced either by Met80, to revert to the native conformation, or by Lys73 or Lys79, to yield one of the conventional alkaline conformers. Evidence is presented to suggest that this group is either a hydroxide ion or Tyr67 rather than a loosely bound Met80.

At alkaline pH, mitochondrial ferricytochromes *c* undergo a reversible conformational change in which Met80 is replaced as a ligand to the heme iron by Lys72, -73, or -79 (*1*−*3*). While the physiological role of this conformational change is uncertain, the pH-linked change in axial ligation involved in this process is reminiscent of ligand exchange processes of heme enzymes of greater structural complexity and provides a useful model for understanding how functional properties of a relatively simple protein can be so dramatically linked to pH (*2*). The alkaline isomerization of ferricytochrome *c* is generally represented as a two-step process as first described by Schejter and co-workers [Scheme 1; (*4*)]. The first step of this mechanism involves deprotonation of a titratable group in the native protein (III-H) with a pK_H of ∼11 to "trigger" the second step, which consists of a ligand exchange reaction (where k_f and k_b are the forward and reverse rate constants, respectively) and the associated structural adjustments of the polypeptide chain. The resulting product is a mixture of alkaline conformational states with His−Lys heme iron coordination that is referred to collectively as state IV (*5*). This mechanism yields the minimum number of parameters necessary to account for the pH dependence of the monoexponential rate constants observed in pH-jump kinetic experiments from neutral pH to pH ∼10 (eq 1):

Scheme 1

$$\text{III-H} \underset{\text{H}^+}{\overset{K_H}{\rightleftharpoons}} \text{III} \underset{k_b}{\overset{k_f}{\rightleftharpoons}} \text{IV}$$

$$k_{obs} = k_b + k_f K_H (K_H + [H^+])^{-1} \quad (1)$$

However, the kinetic profiles of pH-jump experiments above this threshold (i.e., pH 10) exhibit a second phase. This biphasic behavior has been interpreted to result from a parallel pathway for the conversion of the native cytochrome to the alkaline conformations (*6, 7*), and this alternate pathway has been suggested to dominate at higher pH. Subsequently, it was proposed that these two phases correspond to the formation and decay of an intermediate species with an absorption maximum near 600 nm (*8, 9*) that possesses a high-spin, possibly five-coordinate, heme iron center. Presumably, this intermediate also forms below pH 10 but at concentrations that are not detectable.

Previous work from this laboratory has established that replacement of the phylogenetically conserved residue Phe82 (Figure 1) of yeast *iso*-1-cytochrome *c* greatly influences the kinetics and thermodynamics of the alkaline conformational change of this protein (*10*). We now report the properties of a yeast *iso*-1-cytochrome *c* variant, Phe82Trp, that exhibits a thermodynamically stable intermediate with a high-spin heme iron center at mildly alkaline pH.

[†] This work was supported by MRC of Canada Operating Grant MT-14021 (to A.G.M.) and a Heisenberg Fellowship from the Deutsche Forschungsgemeinschaft (to P.H.). The NMR spectrometer was supported by MRC of Canada Maintenance Grant ME-7826 (to Prof. P. R. Cullis).

* Author to whom correspondence should be addressed at the Department of Biochemistry and Molecular Biology, University of British Columbia, Vancouver, British Columbia V6T 1Z3, Canada. Telephone: 604-822-3719; Fax: 604-822-6860; E-mail: mauk@interchg.ubc.ca.

[‡] University of British Columbia.

[§] Present address: Department of Chemistry, Stanford University, Stanford, CA 94305-5080.

[||] Max-Planck-Institute für Strahlenchemie.

10.1021/bi001095k CCC: $19.00
Published on Web 07/08/2000

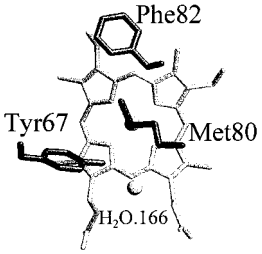

FIGURE 1: The active site structure of yeast *iso*-1-ferricytochrome *c* showing selected residues and a conserved water molecule distal to the heme.

MATERIALS AND METHODS

Protein Preparation. Site-directed mutagenesis of the Cys102Thr variant of the yeast *iso*-1-cytochrome *c* gene (*CYC*1) in the vector pING4 to encode for Trp at position 82 has been described previously (*11*). The additional substitution of Cys102 with Thr in this variant and in the reference "wild-type" protein used in this work for control experiments precludes formation of dimeric forms of the cytochrome and greatly diminishes the rate of autoreduction of the ferricytochrome (*12*). The variant and wild-type proteins were expressed in the yeast *Saccharomyces cerevisiae* strain GM3C-2 and purified by cation exchange chromatography with an FPLC system fitted with a Mono-S HR 10/10 column (Pharmacia Biotech) (*13*). Cytochrome *c* solutions were concentrated by centrifugal ultrafiltration (Centriprep-10 or Centricon-10 units, Millipore), and protein concentrations were determined spectrophotometrically at pH 6.0 with the extinction coefficient of horse heart cytochrome *c* [$\epsilon_{410} = 106.1$ mM^{-1} cm^{-1}, pH 7.0 (*14*)]. Solution pH was determined with a Radiometer Model PHM84 pH meter fitted with a Radiometer Model 2321 combination electrode or an Aldrich microcombination electrode (no. Z 11 343-3). For solutions prepared in D_2O, the pH values quoted are direct meter readings and are, therefore, denoted as pH*.

Kinetic Studies. pH-jump kinetic experiments were performed at 25.0 °C with an Olis RSM-1000 stopped-flow spectrophotometer (Bogart, GA) equipped with a 2 cm path length sample chamber. Spectra (~490−720 nm, 0.7 nm spectral resolution) were recorded at 1 ms intervals, and the resulting data were analyzed with the singular value decomposition algorithm provided by Olis. Alternatively, single-wavelength reaction profiles were extracted and fitted to the appropriate exponential functions. Protein samples (~10 μM ferricytochrome *c* in 0.1 M sodium chloride, pH 5.8) were mixed rapidly with 40 mM buffer solutions of MES[1] (pH 6.5), sodium phosphate (pH 6.9, 7.1, 7.5), TAPS (pH 8.0, 8.7), sodium borate (pH 9.0, 9.5), and CAPS (pH 10.0, 10.1, 10.3). The ionic strength of each of these solutions was adjusted to 0.1 M by addition of the appropriate amount of sodium chloride.

Electronic Spectroscopy. UV/Visible absorption spectra (260−700 nm, 0.5 nm spectral resolution) were recorded at 25.0 °C with a Cary 300 spectrophotometer. Protein samples (~10−100 μM ferricytochrome *c*) were prepared in 100 mM sodium chloride, and the pH was adjusted to the desired value by addition of 0.1 M sodium hydroxide or hydrochloric acid.

Magnetic circular dichroism (MCD) spectra (300−700 nm, 25 °C) were collected with a Jasco Model J720 spectropolarimeter equipped with a 1.5 T electromagnet (Alpha Magnetics) which was fitted with a water-jacketed cell holder. Protein samples (~10 μM ferricytochrome *c*) were prepared as above and were measured with a 1 cm path length cuvette. All spectra are corrected for the background CD signal prior to smoothing using the algorithm available in the Jasco software.

Nuclear Magnetic Resonance Spectroscopy. One-dimensional ^{1}H NMR spectra were recorded with a Bruker MSL-200 spectrometer operating in the quadrature detection mode at 200.13 MHz. Protein samples (2−3 mM ferricytochrome *c*, 400 μL) were prepared in a solution of sodium phosphate and sodium borate buffers (25 mM each) in D_2O. The pH was adjusted to the desired value (6−11) with ~1 M NaOD or D_3PO_4. Spectra (4000−8000 transients) were obtained with a superWeft pulse sequence (*15*) and a recycle delay of 220 ms. The residual water resonance was assigned a chemical shift of 4.63 ppm with respect to DSS.

Electron Paramagnetic Resonance Spectrometry. X-band (~9.5 GHz) EPR spectra were obtained at 10 K with a Bruker Model ESP-300E spectrometer equipped with an Oxford Instruments ESR900 continuous flow cryostat, an ITC4 temperature controller, and a Hewlett-Packard 5352B microwave frequency counter. Microwave power was ~0.5 mW, the modulation frequency was 100 kHz, and the modulation amplitude was 1 mT. Protein samples (~2 mM ferricytochrome *c*, 200 μL) included MES and CAPS buffers (25 mM each) and 50% glycerol (v/v) as a glassing agent. The pH was adjusted by titration with 1 M NaOH (vide supra), measured with the microcombination electrode, and the samples were frozen immediately in liquid nitrogen prior to transfer to the sample cavity.

Resonance Raman Spectroscopy. Spectra of the marker band region (1300−1700 cm^{-1}) were collected at ~25 °C with the excitation line of a Kr^+ laser (413 nm, ~25 mW at the sample) and a double monochromator which was equipped with a photon counting system. The spectroscopic resolution and data point increment were 2.8 and 0.2 cm^{-1}, respectively, and a total accumulation time of ~10 s per data point was used through repeated scanning to improve the signal-to-noise ratio. During the course of each experiment, the reproducibility of the monochromator setting (~0.1 cm^{-1}) was verified by repeated calibration against the position of the laser line. Protein samples (15−28 μM ferricytochrome *c* in 150 mM sodium or potassium phosphate buffer) included a catalytic amount of bovine cytochrome *c* oxidase (<100 nM) to revert photoreduction. All other experimental details have been described at length elsewhere (*16*, *17*).

Single-scan spectra were combined only when careful comparison failed to reveal significant differences among them. The background scattering was removed by polynomial subtraction, and features attributable to ferrocytochrome *c* were subtracted. Each spectrum was then analyzed interactively with a component analysis routine that simulates spectra rather than individual bands (*16*). Unless otherwise stated, the spectra of various structural conformers determined for the wild-type protein, which were derived by

[1] Abbreviations: CAPS, 3-(cyclohexylamino)-1-propanesulfonic acid; CT, charge transfer; DSS, 2,2-dimethyl-2-silapentane-5-sulfonate; MES, 2-(*N*-morpholino)ethanesulfonic acid; MOPS, 3-(*N*-morpholino)propanesulfonic acid; TAPS, *N*-tris(hydroxymethyl)methyl-3-aminopropanesulfonic acid; SHE, standard hydrogen electrode.

component analysis (*17*), were used to analyze the spectra of the Phe82Trp variant.

Electrochemistry. Cyclic voltammograms were obtained at a gold electrode (4 mm diameter) modified with 4,4′-dithiodipyridine as described previously (*18*−*20*). A nonisothermal, two-compartment glass cell was used to maintain a saturated calomel reference electrode (Radiometer, K401) at 25.0 °C in one compartment and to vary the temperature of the sample [ferricytochrome *c* (∼0.3 mM) in 5 mM each MES, MOPS, and TAPS buffers, and 95 mM NaCl] in the other. The protein samples were purged by bubbling the sample solution extensively with humidified Ar or N_2 gas that had been passed through an oxygen-scavenging catalyst before measurement. The sample cell assembly was housed within a Faraday cage to minimize electrostatic interference from external sources. Potentials and sweep rates were controlled with an Ursar Electronics potentistat (Oxford, U.K.) which was interfaced to a microcomputer equipped with a National Instruments Model AT-MIO-16x analog/digital converter board for data collection.

Spectroelectrochemical measurements were performed at 25 °C with an optically transparent thin-layer electrode (OTTLE, ∼0.02 cm path length) (*21*). Protein samples (∼250 μM cytochrome in 20 mM TAPS buffer, pH 8.5, 80 mM sodium chloride) included the mediators 2,6-dichloroindophenol (TCI America, Portland, OR) and $[Ru(NH_3)_6]Cl_3$ (Strem Chemicals) (25 μM each). Catalytic amounts of catalase (Sigma #C100) and *Rhus vernucifera* laccase were added to remove peroxides and oxygen. In each case, the calomel reference electrode (Radiometer Model K401) was standardized against quinhydrone, and potentials are referenced with respect to the SHE (*22*).

RESULTS

Kinetics of the Alkaline Conformational Transition. The time-resolved changes in the electronic spectrum of wild-type yeast *iso*-1-ferricytochrome *c* following a rapid change in pH from 6 to 11.5 are shown in Figure 2A. During the first phase of the reaction, the increasing absorbance of a band near 600 nm reflects the formation of an intermediate high-spin heme iron species which then decays into the alkaline conformers of the cytochrome [states IV and V according to Theorell and Åkesson (*5*)]. A variety of yeast cytochrome *c* variants (e.g., Lys79Ala, Lys73Ala, but not Tyr67Phe) also exhibit this behavior (data not shown). Upon increasing the pH from 5.8 to 8.5, the spectrum of the Phe82Trp variant changes in a similar manner (Figure 2B,C). However, the response of this protein differs from that of the wild-type cytochrome in that (i) the 600 nm band is observed in all pH-jump experiments regardless of the pH, (ii) the amplitude changes of this band are greater for the variant, and (iii) at intermediate pH values a significant residual absorbance persists at 600 nm long after the pH-jump (vide infra).

The pH dependence of the rate constants for the formation and decay of the high-spin species of the variant is shown in Figure 3. The rate constant of the faster phase of the reaction decreases with increasing pH, reaches a minimum near pH 8.5, and then increases as pH is increased further. Kihara et al. and Saigo have reported that cytochromes *c* from a variety of higher eukaryotes exhibit similar behavior

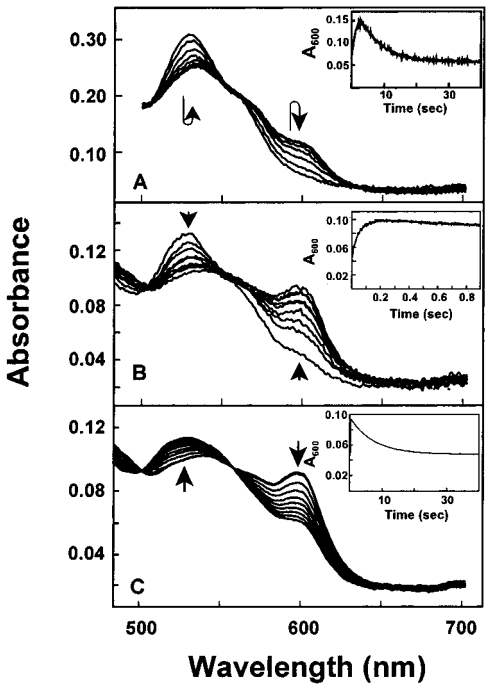

FIGURE 2: Rapid scan kinetic traces of pH-jump kinetics experiments with wild-type yeast *iso*-1-ferricytochrome *c* (pH 6→11.5; panel A) and the variant Phe82Trp (pH 5.8→8.5; panels B and C). The spectra in panel B were collected during the first second (no averaging), and the spectra in panel C were collected over the course of a minute (average of 62 scans/spectrum). The inset in each panel reflects the absorbance at 600 nm as a function of time.

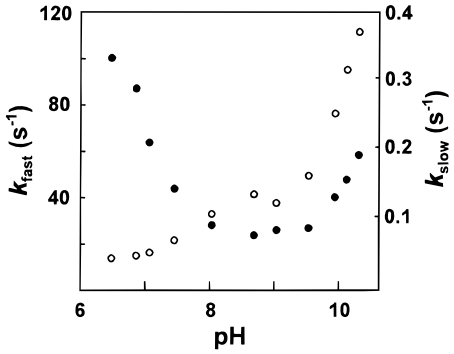

FIGURE 3: pH dependence of the observed rate constants for the formation (●, left scale) and decay (○, right scale) of the A_{600} band in pH-jump kinetic experiments with the Phe82Trp variant of yeast *iso*-1-cytochrome *c* (25.0 °C).

(*6*, *9*). In these cytochromes, the rate constants are comparable (30−100 s^{-1}) to those of the Phe82Trp variant, but this faster phase was not reported to occur below pH 10, and the minimum rate constant occurs at pH ∼11 when state V of cytochrome *c* begins to be populated.

Electronic Absorption Spectroscopy of the Phe82Trp Variant. Below pH 6, the weak absorbance band near 695 nm in the spectrum of the variant is evidence that this cytochrome adopts a native conformation with His−Met coordination (Figure 4) (*23*−*26*). With increasing pH (6.5−8.4), the spectra of this variant form an isosbestic point near 629 nm, indicating that only two species are present within this range of pH. The band emerging above 600 nm with increasing pH reveals that the high-spin heme iron observed in the pH-jump experiments is thermodynamically stable at 25 °C and 0.1 M sodium chloride. Under these conditions, maximum high-spin character is achieved at pH ∼8.5.

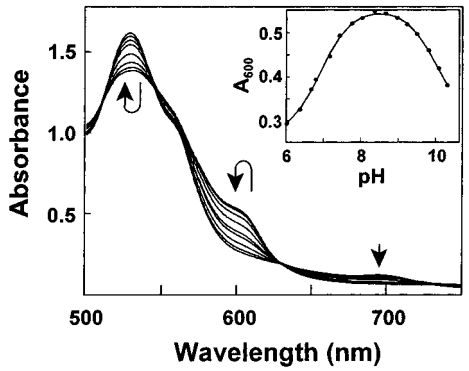

FIGURE 4: Spectrophotometric pH titration of the Phe82Trp variant of yeast *iso*-1-ferricytochrome *c* (100 mM NaCl, 25.0 °C). The inset shows the variation of the absorbance at 600 nm with pH and the fitted curve for a model for the deprotonation of two species.

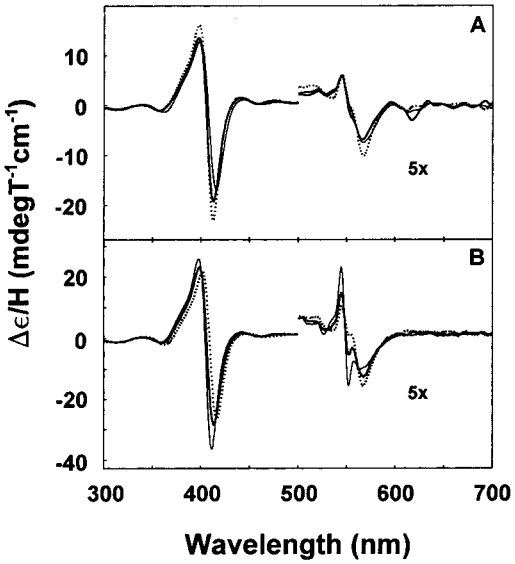

FIGURE 5: MCD spectra (1 T, 25 °C) of wild-type yeast *iso*-1-ferricytochrome *c* (B) and the Phe82Trp variant (A) measured at at pH ~5.9 (• • •), ~8.5 (—), and ~10 (- - -). The sharp *A*-term at ~550 nm in the spectra of the wild-type protein corresponds to a small amount of ferrocytchrome *c* in the sample.

Further increases in pH cause the heme iron of the variant to revert to a low-spin configuration presumably as a result of the formation of the conventional alkaline species of the protein (*27*). The spectra collected above pH 8.5 do not conform to the isosbestic point at 629 nm. Therefore, at least a third species becomes populated in this range of pH. Fitting the A_{600} values as a function of pH to a model for the deprotonation of two groups yields pK_{app} values of 6.98(3) and 9.95(8) for the formation and decay of the high-spin species respectively (Figure 4, inset). Note, however, that in the presence of buffer salts (sodium phosphate and sodium borate buffers, 25 mM each) and/or at higher protein concentrations (~2 mM), ^{1}H NMR spectroscopy reveals that two alkaline forms of the variant are present in the sample even at pH* ~7.0 (vide infra).

The MCD (1 T) spectrum of the variant measured as a function of pH is shown in Figure 5. These spectra are very similar to those of the wild-type cytochrome (data not shown) except for the negative Cotton effect at 617 nm. As expected, this feature reaches maximum intensity near pH 8.5, and it resembles a CT band that is found in the spectrum of alkaline metmyoglobin [616 nm (*28*)]. The sharp *A*-term just below

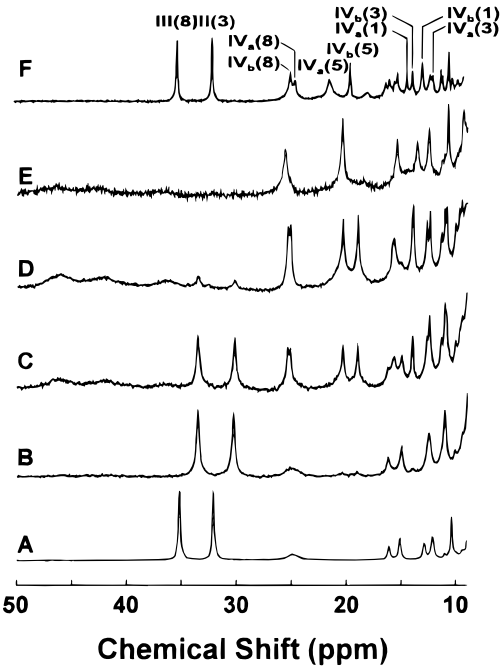

FIGURE 6: Hyperfine-shifted ^{1}H NMR spectra of wild-type yeast *iso*-1-ferricytochrome *c* and the Phe82Trp variant (20 °C): (A) wild-type cytochrome, pH* 7.0; (F) wild-type cytochrome, pH* 9.2; (B) variant, pH* 5.6; (C) variant, pH* 6.5; (D) variant, pH* 8.5; and (E) variant, pH* 10.9. Roman numerals indicate the conformational state of the cytochrome (*4*), subscripts refer to the alkaline form of the protein (i.e., a, Lys73-bound; b, Lys79-bound), and the numbers in parentheses refer to the heme methyl group protons that give rise to the resonance.

550 nm in the corresponding spectra of the wild-type protein is attributable to a small fraction of the sample that is present in the ferrous form.

^{1}H NMR Spectroscopy. A comparison of the hyperfine-shifted ^{1}H NMR spectra of the wild-type and variant cytochromes as a function of pH* is shown in Figure 6. At pH* 5.6, the spectrum of the variant closely resembles that of the wild-type protein measured at pH* 7.0 (Figure 6B and 6A, respectively). Notably, the resonances associated with the His18 ϵ1-H and β-CH (~24.9 and ~15.1 ppm, respectively) and the propionate 7α-CH_2 (~16.1 ppm) appear with the same chemical shift (*29*). However, some spectroscopic differences associated with protons on the distal side of the heme near the site of the mutation are encountered. The peak corresponding to the Met80 ϵ-CH_3 protons (not shown), for example, appears at ~-23.0 ppm ($\Delta\delta$ +0.7 ppm relative to wild-type cytochrome *c*). The signals that correspond to the heme 8- and 3-methyl group protons shift to 33.5 ($\Delta\delta$ −1.7) and 30.4 ($\Delta\delta$ −1.8) ppm, respectively.

In the spectrum measured at pH* 6.5 (Figure 6C), spectroscopic features of the alkaline conformers of the variant (a doublet at ~24 ppm, and two singlets at 20 and 19 ppm) begin to emerge together with three broad resonances between 38 and 47 ppm (Figure 6C−E). Above pH* 10, these new broad features become less prominent in the spectrum and are, therefore, assigned to the high-spin species of the protein. At even higher pH, another shift in the conformational equilibria of the variant occurs, as the Lys73-bound alkaline conformer of the cytochrome becomes the sole low-spin species present at pH* 10.9 (Figure 6E).

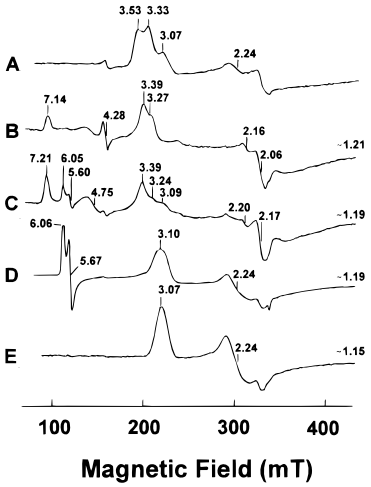

FIGURE 7: X-band EPR spectra of wild-type yeast *iso*-1-ferricytochrome *c* and the Phe82Trp variant: (A) wild-type cytochrome, pH 10.5; (B) variant, pH 10.8; (C) variant, pH 8.3; (D) variant, pH 6.3; and (E) wild-type cytochrome, pH 6.0.

EPR Spectroscopy. Depending on pH, the EPR spectra of the variant of ferricytochrome *c* exhibit features of multiple species (Figure 7). Near neutral pH, the signals at $g_z = 3.10$, $g_y = 2.24$, and $g_x \sim 1.19$ correspond to the native conformation of the protein. The signals $g_z \sim 6.06$ and $g_y \sim 5.67$ correspond to a highly rhombic species which disappears with increasing pH and which probably result from an acidic conformational equilibrium of the protein or a cryogenic artifact introduced during sample preparation. These signals were also encountered in the EPR spectrum of the Phe82Lys variant of yeast *iso*-1-ferricytochrome *c* that was measured under similar conditions (Rosell et al., in preparation). For this latter variant, this rhombic signal also diminishes with increasing pH.

The signals that appear at $g_z \sim 3.39$ and 3.24 in the spectrum collected at pH 8.3 (Figure 7C) correspond to the alkaline conformers of the protein (*27*). With increasing pH, these species become the dominant forms of the protein to the detriment of an unusual form of ferricytochrome *c* which reaches maximum concentration near pH 8.5. This species is also characterized by a highly rhombic spectrum with $g \sim 7.14-7.21$ and ~4.75. Note that the His93Tyr variant of horse heart myoglobin exhibits very similar EPR parameters [$g \sim 7.13$ and 4.89 (*30*)]. In this protein, the proximal phenolate of Tyr93 coordinates the ferriheme iron to produce a pentacoordinate species. However, although the electronic spectrum of this myoglobin variant also exhibits a transition just above 600 nm, the electronic spectrum of the myoglobin variant differs from that of the wild-type protein while the spectrum of the native cytochrome variant is the same as that of the wild-type cytochrome.

Resonance Raman Spectroscopy. The marker band region of the resonance Raman spectrum of the variant measured at pH 8.3 is compared to that of the wild-type cytochrome in Figure 8 (panels B and A, respectively). The most significant spectroscopic difference between these two proteins that is evident in these spectra is the peak centered at 1477.5 cm^{-1} in the spectrum of the variant, which corresponds to the ν_3 mode of a high-spin, hexacoordinate heme iron species. Using the component analysis parameters of wild-type cytochrome (*17*) to fit the components present

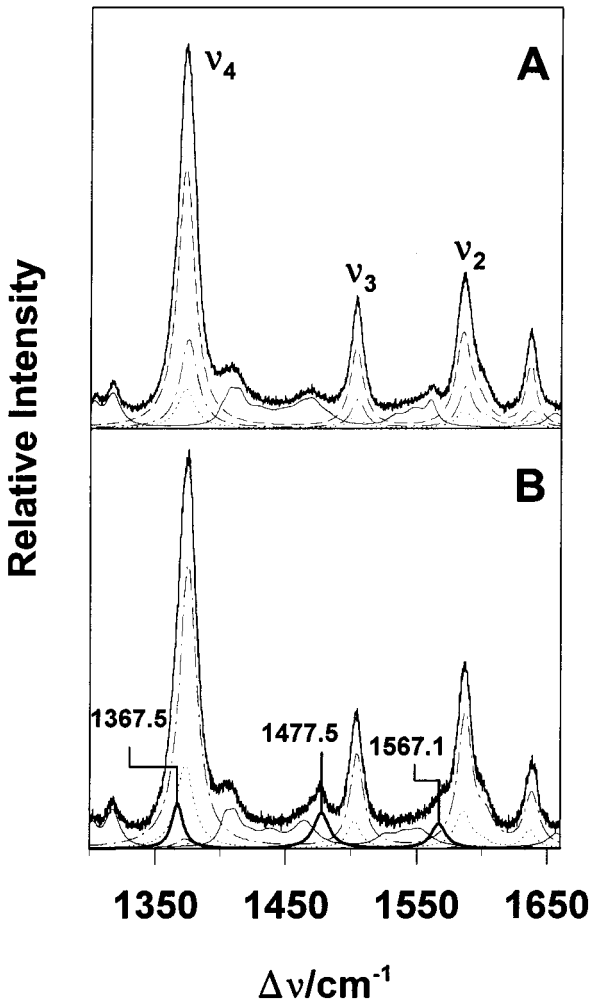

FIGURE 8: Resonance Raman spectra in the marker band region of yeast *iso*-1-ferricytochrome *c* (pH 8.3): (A) wild-type cytochrome *c*; (B) Phe82Trp cytochrome *c*. The contributions from the various conformational species determined by component analysis are indicated as follows: native III (- - -); Lys73-bound IV_a (— · —), Lys79-bound IV_b (— —), hexacoordinate high-spin (—).

in the spectrum of the variant yields two other modes in this region (ν_2 and ν_4 at 1567.1 and 1367.5 cm^{-1}, respectively) which are consistent with this assignment (*31*). From this analysis, it is estimated that approximately 10% of the protein is present in this high-spin state at pH 8.3. The remainder of the protein is present either in the native conformation or as alkaline cytochrome *c*.

Electrochemistry. At pH 6.6, the electrochemistry of the variant at a 4,4′-dithiodipyridine-modified gold electrode is quasi-reversible at all temperatures (5−35 °C) with peak-to-peak separations within 1−2 mV of the expected value at any given temperature. A reduction potential of 266 mV vs SHE is within the range of other Phe82Xxx variants [Xxx = Gly, Leu, Ser, Ala, Tyr, Ile: 247−290 mV vs SHE (*13*, *32*)] and suggests that replacement of Phe82 with Trp does not alter the heme cavity significantly more than any of the other mutations (e.g., *33*−*35*). With Trp at position 82, the temperature dependence of the reduction potential of the variant differs from that of the wild-type cytochrome largely as the result of an entropic effect which is, however, compensated partially by an enthalpic contribution (Table 1).

Table 1: Electrochemical Properties of Wild-Type Yeast *iso*-1-Cytochrome *c* and the Variant Phe82Trp

protein	wild-type	Phe82Trp
E_m (mV vs SHE)[a]	290	266
ΔG (kcal mol^{-1})	−6.7	−6.2
ΔH (kcal mol^{-1})	−14.1	−14.5
ΔS (e.u.)	−9.1	−12.4

[a] pH 6.0, 25.0 °C, μ = 0.1 M KCl, ν = 20 mV/s.

Attempts to measure the reduction potential of the high-spin species by cyclic voltammetry were unsuccessful presumably owing to the change in the spin-state that is expected to accompany reduction or oxidation and owing to the relatively low abundance of this form of the cytochrome. At pH 8.5, spectroelectrochemical measurements yielded a reduction potential of 131 mV vs SHE, but the slopes of the Nernst plots were consistently 75 mV, reflecting the conformational heterogeneity of the sample at this pH.

DISCUSSION

In the three-dimensional structure of cytochrome *c*, Phe82 is located on the distal side of the heme where it comprises part of the heme binding pocket (*36*−*47*). The phenyl ring of this residue is adjacent to pyrrole rings B and C (within ∼4.3 Å) and is almost coplanar with them (Figure 1). This location combined with the phylogenetic invariance of Phe82 in the sequences of mitochondrial cytochromes *c* (*12*) led to selection of this site as the first target for site-directed mutagenesis of this protein (*48*) and to the eventual replacement of this residue by all 19 naturally occurring amino acids (*11*). Of these variants, those with Gly, Ser, Leu, Ala, Tyr, Ile, Met (*13*, *32*−*35*, *49*, *50*), and His (*51*−*53*) have been characterized to varying degrees.

A variety of spectroscopic results establish that the active site of the Phe82Trp variant adopts the native structure at mildly acidic pH (i.e., pH ≤6): (i) the weak charge-transfer band near 695 nm characteristic of His−Met coordination is present (*23*−*26*); (ii) the *A*-term in the Soret region of the CD spectrum is observed (not shown) (*54*, *55*); and (iii) the EPR spectrum is that of native ferricytochrome *c* (*56*). Moreover, the midpoint reduction potential of this variant is comparable to that of other Phe82 variants (*13*, *32*). The one-dimensional ^{1}H NMR spectrum indicates that some features associated with the heme group and Met80 are perturbed slightly in the variant. However, these differences are not sufficient to suggest that the larger indole group introduces gross structural changes. At high pH (∼10), NMR and resonance Raman spectra of the variant also indicate that two alkaline conformations with His−Lys heme coordination are populated as a result of two independent alkaline isomerizations. The similarity of both the native and alkaline isomers of the variant to the corresponding forms of the wild-type cytochrome lead us to conclude that the structural reorganization in both proteins monitored by pH-jump kinetic experiments reflects the same processes. The characteristic that distinguishes the Phe82Trp variant is the thermodynamic stability of a conformational intermediate that occurs prior to the typical alkaline conformers.

Mechanism of the Alkaline Conformational Transition. In the simplified mechanism of the alkaline isomerization of ferricytochrome *c* (Scheme 1), the ionization of a titratable group (pK_H) triggers the subsequent replacement of the Met80 ligand (pK_C) (*3*). However, a more complete description of this process includes at least one intermediate in which neither Met80 nor a Lys residue is coordinated to the metal center (*7*−*9*). This species is a common precursor to both alkaline forms of the yeast cytochrome and, perhaps, also of state V, which forms at very high pH (≥10.5). Such an intermediate could be pentacoordinate or could possess a hexacoordinate heme iron in which a water molecule or a residue from the distal side of the heme pocket binds transiently to the metal center.

The electronic spectrum of the variant of yeast *iso*-1-cytochrome *c* exhibits features at pH ∼8.5 that are observed transiently in the spectrum of the wild-type protein upon rapidly increasing solution pH to high values. A similar spectrum is observed for the Lys73Ala/Lys79Ala variant (expressed in yeast so that Lys72 is trimethylated) at high pH (e.g., ∼10.5), conditions where Met80 is expelled from the iron coordination sphere but neither Lys73 nor Lys79 is available to coordinate the heme iron. This spectroscopic similarity suggests that the thermodynamically stable, high-spin form of the variant is identical or related to an intermediate of the alkaline isomerization of ferricytochromes *c*.

Identity of the Sixth Ligand. The resonance Raman experiments indicate that the stable intermediate exhibited by the Phe82Trp variant is a hexacoordinated heme iron species and raise the question of the identity of the sixth iron ligand. One possible candidate is the internal water molecule that is conserved in the X-ray crystal structures of cytochromes *c*, H_2O.166 (e.g., PDB accession no. 2YCC). Replacement of Phe82 with Trp introduces a functional group into the heme cavity (i.e., the indole nitrogen) that can serve as a hydrogen bond donor to a coordinated water molecule and thus stabilize the $Fe^{III}-OH_x$ bond. This possibility is supported by features in the electronic, MCD, and ^{1}H NMR spectra of the variant that closely resemble those of hydroxymetmyoglobin (*28*, *57*). In this myoglobin derivative, the hydroxide bound to the iron also forms a hydrogen bond with the ϵ-2 nitrogen of the distal histidyl residue. Note that in the spectrum of the Met80Ala variant of yeast cytochrome *c* in which hydroxide is coordinated to the heme iron, the charge-transfer maximum occurs at ∼625 nm rather than ∼600 nm (*58*, *59*). The blue shift of this band in spectra of the Phe82Trp variant supports the assumption that a hydrogen bond to a His or the indole ring of Trp is involved.

Alternatively, Tyr67 may provide the sixth ligand in the conformational intermediate exhibited by the variant. Electronic and resonance Raman spectra of human Hb variants with distally coordinated Tyr residues (HbM Saskatoon and HbM Boston) and of His64Tyr variants of Mb exhibit characteristics (*60*, *61*) that agree with the electronic spectra and the component analysis of the resonance Raman spectra presented here for the cytochrome variant. Crystallographic and XANES analyses of the myoglobin variants (*63*, *64*) have shown that the ferric form of this protein is heaxacoordinate with Tyr(E7) providing the distal ligand. Under certain conditions, the EPR spectra of these proteins are characterized by highly rhombic signatures at $g \sim 6.7$ and 5.7 (*61*, *64*). These results differ from those obtained for the Phe82Trp variant which, according to EPR measurements, resembles more closely the horse heart myoglobin variant

in which the proximal His(F8) residue is replaced with Tyr. Such Mb variants exhibit a pentacoordinate, high-spin heme iron with a proximally coordinated Tyr ligand (*30*). The involvement of Tyr67 in formation of the kinetic intermediate would explain the absence of the transient 600 nm charge-transfer band upon rapidly increasing the pH of the yeast Tyr67Phe cytochrome variant from 6 to ~12. Again, Trp82 could form a hydrogen bond with and thereby stabilize a coordinated Tyr67 ligand.

Relationship to Folding Intermediates and Other Spectroscopic Species of Ferricytochrome c. As noted above, the Lys73Ala/Lys79Ala variant exhibits spectroscopic features in electronic (*27*) and resonance Raman spectra (*17*) that are similar to those of the variant, and, by association, to those of the intermediate of the alkaline conformational transition of these proteins.Interestingly, treatment of equine ferricytochrome *c* with triethylphosphine gold(I) chloride has been shown also to induce similar spectroscopic changes [a charge-transfer band at 600 nm and a highly rhombic EPR signature with $g \sim 6.4$ and 5.1 (*65*)] to those observed in the present study. Whether or not these forms of cytochrome *c* are related to either the reaction intermediate and/or the trapped intermediate described in this work remains to be determined.

A role for ligand exchange in ferricytochrome *c* structural dynamics has also arisen from studies of folding and unfolding of the protein (*66*−*72*). From this work, His26 and His33 have been reported to be capable of replacing Met80 (*66*−*68*) in partially unfolded forms of the protein. In addition, introduction of His residues at various positions in a variant of yeast *iso*-1-ferricytochrome *c* from which the native His residues have been removed results in variants in that exhibit new conformers with bis-hisitidine axial ligation when partially unfolded (*69, 71, 72*). Interestingly, related studies of the His-depleted variant of the yeast cytochrome revealed that the α-amino group can also replace Met80 upon partial unfolding of the protein (*70*). Although there has been no report of coordination of a lysyl residue resulting from such studies so far, it seems reasonable nevertheless to expect that such an intermediate could form under appropriate conditions of pH, temperature, and electrolyte composition.

In summary, the pH-linked conformational behavior of the Phe82Trp cytochrome *c* variant is distinct from that of other cytochrome variants studied previously in that a thermodynamically stable intermediate is observed at moderately alkaline pH. This structural intermediate exhibits spectroscopic characteristics reminiscent of a transiently stable intermediate species that is normally observed only during pH-jump kinetic experiments with the wild-type cytochrome or other variants. Although the structural factors responsible for the thermodynamic stability of this intermediate remain to be delineated, it seems reasonable to suggest that the relatively large size of the indole side chain of Trp82 inhibits the otherwise kinetically facile structural rearrangement that accompanies titration of ferricytochrome *c* in this range of pH. Functional and spectroscopic characterization of this stabilized intermediate as initiated here offers the potential to define the structural reorganization pathway involved in this conformation change in considerable depth.

ACKNOWLEDGMENT

We thank Professor Pieter R. Cullis for access to the NMR spectrometer.

REFERENCES

1. Rosell, F. I. Ferrer, J. C., and Mauk. A. G. (1998) *J. Am. Chem. Soc. 120*, 11234−11245.
2. Pollock, W. B., Rosell, F. I., Twitchett, M. B., Dumont, M. E., and Mauk, A. G. (1998) *Biochemistry 37*, 6124−6131.
3. Banci, L., Bertini, I., Spyroulias, G. A., and Turano, P. (1998) *Eur. J. Inorg. Chem. 5*, 583−591.
4. Davis, L. A., Schejter, A., and Hess, G. P. (1974) *J. Biol. Chem. 249*, 2624−2632.
5. Theorell, H., and Åkesson, A. (1941) *J. Am. Chem. Soc. 63*, 1804−1811.
6. Kihara, H., Saigo, S., Nakatani, H., Hiromi, K., Ikeda-Saito, M., and Iizuka, T. (1976) *Biochim. Biophys. Acta 430*, 225−243.
7. Hasumi, H. (1980) *Biochim. Biophys. Acta 626*, 265−276.
8. Lambeth, D. O., Campbell, K. L., Zand, R., and Palmer, G. (1973) *J. Biol. Chem. 248*, 8130−8136.
9. Saigo, S. (1981) *Biochim. Biophys. Acta 669*, 13−20.
10. Pearce, L. L., Gärtner, A. L., Smith, M., and Mauk, A. G. (1989) *Biochemistry 28*, 3152−3156.
11. Inglis, S. C., Guillemette, J. G., Johnson, J. A., and Smith, M. (1991) *Protein Eng. 4*, 569−574.
12. Cutler, R. L., Pielak, G. J., Mauk, A. G., and Smith, M. (1987) *Protein Eng 1*, 95−99.
13. Rafferty, S. P., Pearce, L. L., Barker, P. D., Guillemette, J. G., Kay, C. M., Smith, M., and Mauk, A. G. (1990) *Biochemistry 29*, 9365−9369.
14. Margoliash, E., and Frohwirt, N. (1959) *Biochem. J. 71*, 570−572.
15. Inubushi, T., and Becker, E. D. (1983) *J. Magn. Reson. 51*, 128−133.
16. Döpner, S., Hildebrandt, P., and Mauk, A. G. (1996) *Spectrochim. Acta 52A*, 573−584.
17. Döpner, S., Hildebrandt, P., Rosell, F. I., and Mauk, A. G. (1998) *J. Am. Chem. Soc. 120*, 11246−11255.
18. Taniguchi, I., Toyosawa, K., Yamaguchi, H., and Yasukouchi, K. (1982) *J. Chem. Soc., Chem. Commun.*, 1032−1033.
19. Taniguchi, I., Toyosawa, K., Yamaguchi, H., and Yasukouchi, K. (1982) *J. Electroanal. Chem. 140*, 187−193.
20. Allen, P. M., Hill, H. A. O., and Walton, N. J. (1984) *J. Electroanal. Chem. 178*, 69−86.
21. Reid, L. S., Taniguchi, V. T., Gray, H. B., and Mauk, A. G. (1982) *J. Am. Chem. Soc. 104*, 7516−7519.
22. Dutton, P. L. (1978) *Methods Enzymol. 54*, 411−435.
23. Schechter, E., and Saludjian, P. (1967) *Biopolymers 5*, 788−790.
24. Eaton, W. A., and Hochstrasser, R. M. (1967) *J. Chem. Phys. 46*, 2533−2539.
25. Hochstrasser, R. (1967) *J. Chem. Phys. 46*, 2533−2539.
26. Smith, D. W., and Williams, R. J. P. (1970) *Struct. Bonding 7*, 1−45.
27. Rosell, F. I., Ferrer, J. C., and Mauk, A. G. (1998) *J. Am. Chem. Soc. 120*, 11234−11245.
28. Sono, M., and Dawson, J. H. (1984) *Biochim. Biophys. Acta 789*, 170−187.
29. Gao, Y., Boyd, J., Williams, R. J., and Pielak, G. J. (1990) *Biochemistry 29*, 6994−7003.
30. Hildebrand, D. P., Burk, D. L., Maurus, R., Ferrer, J. C., Brayer, G. D., and Mauk, A. G. (1995) *Biochemistry 34*, 1997−2005.
31. Parthasarathi, N., Hansen, C., Yamaguchi, S., and Spiro, T. G. (1987) *J. Am. Chem. Soc. 109*, 3865−3871.
32. Rafferty, S. P., Guillemette, J. G., Berghuis, A. M., Smith, M., Brayer, G. D., and Mauk, A. G. (1996) *Biochemistry 35*, 10784−10792.
33. Louie, G. V., and Brayer, G. D. (1989) *J. Mol. Biol.* 210, 313−322.

34. Louie, G. V., Pielak, G. J., Smith, M., and Brayer, G. D. (1988) *Biochemistry 27*, 7870−7876.
35. Lo, T. P., Guillemette, J. G., Louie, G. V., Smith, M., and Brayer, G. D. (1995) *Biochemistry 34*, 163−171.
36. Dickerson, R. E., Takano, T., Eisenberg, D., Kallai, O. B., Samson, L., Cooper, A., and Margoliash, E. (1971) *J. Biol. Chem. 246*, 1511−1535.
37. Bushnell, G. W., Louie, G. V., and Brayer, G. D. (1990) *J. Mol. Biol. 214*, 585−595.
38. Sanishvili, R., Volz, K. W., Westbrook, E. M., and Margoliash, E. (1995) *Structure 3*, 707−716.
39. Takano, T., Kallai, O. B., Swanson, R., and Dickerson, R. E. (1973) *J. Biol. Chem. 248*, 5234−5255.
40. Takano, T., Trus, B. L., Mandel, N., Mandel, G., Kallai, O. B., Swanson, R., and Dickerson, R. E. (1977) *J. Biol. Chem. 252*, 776−785.
41. Swanson, R., Trus, B. L., Mandel, N., Mandel, G., Kallai, O. B., and Dickerson, R. E. (1977) *J. Biol. Chem. 252*, 759−775.
42. Tanaka, N., Yamane, T., Tsukihara, T., Ashida, T., and Kakudo, M. (1975) *J. Biochem. (Tokyo) 77*, 147−162.
43. Ochi, H., Hata, Y., Tanaka, N., Kakudo, M., Sakurai, T., Aihara, S., and Morita, Y. (1983) *J. Mol. Biol. 166*, 407−418.
44. Ashida, T., Tanaka, N., Yamane, T., Tsukihara, T., and Kakudo, M. (1973) *J. Biochem. (Tokyo) 73*, 463−465.
45. Berghuis, A. M., and Brayer, G. D. (1992) *J. Mol. Biol. 223*, 959−976.
46. Louie, G. V., Hutcheon, W. L., and Brayer, G. D. (1988) *J. Mol. Biol. 199*, 295−314.
47. Louie, G. V., and Brayer, G. D. (1990) *J. Mol. Biol. 214*, 527−555.
48. Pielak, G. J., Mauk, A. G., and Smith, M. (1985) *Nature 313*, 152−154.
49. Barker, P. D., and Mauk, A. G. (1992) *J. Am. Chem. Soc. 114*, 3619−3624.
50. Liang, N., Mauk, A. G., Pielak, G. J., Johnson, J. A., Smith, M., and Hoffman, B. M. (1988) *Science 240*, 311−313.
51. Schejter, A., Taler, G., Navon, G., Liu, X. J., and Margoliash, E. (1996) *J. Am. Chem. Soc. 118*, 477−478.
52. Feinberg, B. A., Liu, X., Ryan, M. D., Schejter, A., Zhang, C., and Margoliash, E. (1998) *Biochemistry 37*, 13091−13101.
53. Hawkins, B. K., Hilgen-Willis, S., Pielak, G. J., and Dawson, J. H. (1994) *J. Am. Chem. Soc. 116*, 3111−3112.
54. Looze, Y., Polastro, E., Deconinck, M., and Leonis, J. (1978) *Int. J. Pept. Protein Res. 12*, 233−236.
55. Santucci, R., and Ascoli, F. (1997) *J. Inorg. Biochem. 68*, 211−214.
56. Palmer, G. in *The Porphyrins* (Dolphin, D., Ed.) pp 313−353, Academic Press, New York.
57. Iizuka, T., and Morishima, I. (1975) *Biochim. Biophys. Acta 400*, 143−153.
58. Bren, K. L. (1996) Ph.D. Dissertation, California Institute of Technology, Pasadena, CA.
59. Twitchett, M. B. (1998) Ph.D. Dissertation, University of British Columbia, Vancouver, B.C., Canada.
60. Nagai, K., Kagimoto, T., Hayashi, A., Taketa, F., and Kitagawa, T. (1983) *J. Am. Chem. Soc. 22*, 1305−1311.
61. Egeberg, K. D., Springer, B. A., Martinis, S. A., and Sligar, S. G. (1990) *Biochemistry 29*, 9783−9791.
62. Nagai, M., Yoneyama, Y., and Kitagawa, T. (1989) *Biochemistry 28*, 2418−2422.
63. Maurus, R., Bogumil, R., Luo, Y., Tang, H. L., Smith, M., Mauk, A. G., and Brayer, G. D. (1994) *J. Biol. Chem. 269*, 2606−2610.
64. Pin, S., Alpert, B., Cortes, R., Ascone, I., Chiu, M. L., and Sligar, S. G. (1994) *Biochemistry 33*, 11618−11623.
65. Otiko, G., and Sadler, P. J. (1980) *FEBS Lett. 116*, 227−230.
66. Elove, G. A., Bhuyan, A. K., and Roder, H. (1994) *Biochemistry 33*, 6925−6935.
67. Yeh, S. R., Takahashi, S., Fan, B., and Rousseau, D. L. (1997) *Nat. Struct. Biol. 4*, 51−56.
68. Colon, W., Wakem, L. P., Sherman, F., and Roder, H. (1997) *Biochemistry 36*, 12535−12541.
69. Godbole, S., and Bowler, B. E. (1997) *J. Mol. Biol. 268*, 816−821.
70. Hammack, B., Godbole, S., and Bowler, B. E. (1998) *J. Mol. Biol. 275*, 719−724.
71. Godbole, S., and Bowler, B. E. (1999) *Biochemistry 38*, 487−495.
72. Godbole, S., Hammack, B., and Bowler, B. E. (2000) *J. Mol. Biol. 296*, 217−228.

BI001095K